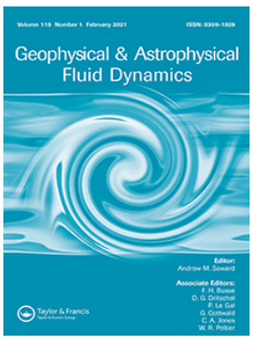

Geophysical & Astrophysical Fluid Dynamics

ISSN: (Print) (Online) Journal homepage: https://www.tandfonline.com/loi/ggaf20

Frictional effects in wind-driven ocean currents

Adrian Constantin

To cite this article: Adrian Constantin (2021) Frictional effects in wind-driven ocean currents, Geophysical & Astrophysical Fluid Dynamics, 115:1, 1-14, DOI: 10.1080/03091929.2020.1748614

To link to this article: https://doi.org/10.1080/03091929.2020.1748614

Published online: 16 Apr 2020.

GEOPHYSICAL & ASTROPHYSICAL FLUID DYNAMICS
2021, VOL. 115, NO. 1, 1–14
https://doi.org/10.1080/03091929.2020.1748614

Taylor & Francis
Taylor & Francis Group

Frictional effects in wind-driven ocean currents

Adrian Constantin

Faculty of Mathematics, University of Vienna, Vienna, Austria

ABSTRACT
Surface ocean currents have a significant influence on the climate and their dynamics depend to a large extent on the behaviour of the vertical eddy viscosity. We present an analytic study of wind-driven surface currents for general depth-dependent vertical eddy viscosities. A novel formulation for Ekman-type flows, that relies of a transformation to polar coordinates, enables us to show that in the Northern Hemisphere the horizontal current profile decays in magnitude and turns clockwise with increasing depth, irrespective of the vertical variations in diffusivity. Using a perturbation approach, we also derive a formula for the deflection angle of the current at the surface from the wind direction and discuss its implications.

ARTICLE HISTORY
Received 10 January 2020
Accepted 25 March 2020

KEYWORDS
Wind-driven current; spiralling horizontal flow; deflection angle

1. Introduction

The ocean covers more than 70% of the Earth's surface and is the largest solar energy collector on Earth. As water can absorb large amounts of heat without a large increase in temperature, the oceans are Earth's largest thermal reservoir, with the upper 3 m of the ocean storing as much heat as the overlying atmosphere (see Gill 2018). Also, more than 80% of the Earth's thermal imbalance due to the anthropogenic forcing has been absorbed by the ocean (see Levitus *et al.* 2012) and the Intergovernmental Panel on Climate Change (IPCC) 5th Assessment Report revealed that the ocean has absorbed 93% of the extra energy from the enhanced greenhouse effect. This is especially relevant since the rate of global warming is determined mainly by the increase of anthropogenic greenhouse gases and the ocean heat uptake, with most of the increase in temperature concentrated in the ocean's upper 100 m (see Levitus *et al.* 2012). Moreover, the rate of warming of the upper ocean is currently larger than that of the deep ocean (see Marshall and Zanna 2014). The tremendous ability to store and release heat over long periods of time gives the ocean a central rôle in stabilising the climate, with the ocean currents helping to counteract the uneven distribution of solar radiation reaching Earth's surface (see Marshall and Plumb 2016). While the thermohaline circulation due to deep-ocean currents has an impact on climate (see Vallis 2005), the heat transport due to surface ocean currents is also a key the factor in regulating the global climate. Surface ocean currents can occur on local to global scales and are typically wind-driven, their effect being mainly confined to the top 400 m of the ocean.

CONTACT Adrian Constantin adrian.constantin@univie.ac.at

Note that the horizontal mass transport induced by wind-drift currents generates vertical movement throughout the upper 1 km of the ocean since these transports converge in some regions and diverge in others, and mass conservation brings about the development of vertical flow to replace or remove the diverging/converging water masses; for example, the convergence occurring throughout the subtropical North Pacific is associated with downwelling, while the divergence in the subpolar North Pacific is related to upwelling (see Talley *et al.* 2011). Even though the horizontal velocities of ocean flows, typically of the order of $1\,\mathrm{m\,s^{-1}}$, are about a factor 10^4 larger than the vertical velocities (see Viúdez and Dritschel 2003), downwelling is a key process in the transfer of energy from the surface to the interior of the oceans (see Roquet *et al.* 2011). Since surface currents can carry warmed or cooled water as far as several thousand kilometres (for example, the warm Gulf Stream in the North Atlantic or the cold Humboldt current in the South Pacific), an apparently small change in just one aspect of the ocean's behaviour can produce major climate variations over large areas. A better conceptual understanding of the generation of surface currents, based on models that represent the main physical processes more realistically, is therefore relevant for climate studies.

Ekman's theory of wind-driven currents (see Ekman 1905) is a cornerstone of physical oceanography, being essential in our understanding of the wind-driven ocean circulation. Yet Ekman's theory relies on a number of idealised assumptions rarely met in reality. Ekman's explicit solution applies to uniform steady wind blowing over a homogeneous ocean having a constant eddy viscosity, with the wind-induced current having the following characteristics (see figure 1):

(i) the surface flow is directed at an angle of 45° *cum sole* to the wind (that is, to the right in the Northern Hemisphere and to the left in the Southern Hemisphere);
(ii) in successively deeper layers the current speed is reduced, and the direction rotates farther away from the wind direction following a spiral;
(iii) the vertically averaged wind-driven motion (Ekman transport) is at 90° to the wind, being to the right/left of the wind direction in the Northern/Southern Hemisphere.

An essential feature of Ekman's approach – that the dominant momentum balance for steady wind-driven currents is between the wind stress, frictional forces and the Coriolis acceleration – breaks down in equatorial regions, where the Coriolis effect due to the Earth's rotation vanishes so that the resulting wind drift current moves azimuthally, in the same direction as the wind (see Basu 2019, Boyd 2018), and where nonlinear effects have to be accounted for (see Henry 2018, Constantin and Johnson 2019b, 2019c). However, in non-equatorial regions, Ekman's precept holds: the wind-driven stress is balanced by the Coriolis force and frictional forces. Indeed, observational evidence for Ekman's solution is provided by the wind-driven currents in the Southern Ocean and in some coastal straits (see Stacey *et al.* 1986, Polton *et al.* 2013, Roach *et al.* 2015). However, some data in non-equatorial regions, while confirming the mass transport to the right of the wind direction and being qualitatively similar to the other two of Ekman's predictions, exhibit noticeable quantitative mismatches, both with regard to the deflection angle of the surface current from the wind direction (with values below 20° and in excess of 50° being reported in Yoshikawa and Masuda 2009) as well as with respect to the turning rate with depth. A depth-dependent eddy viscosity is typically essential to overcome the inconsistency

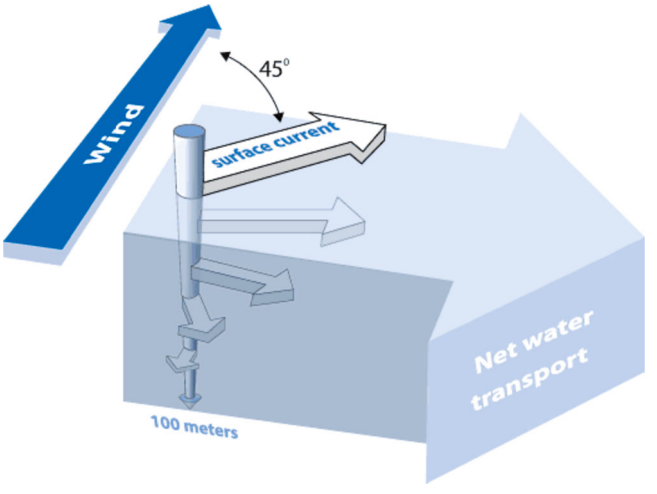

Figure 1. Depiction of Ekman's classical solution: while the surface current is deflected by 45°, each deeper layer in the water column is deflected slightly less, which results in a spiral pattern decaying exponentially with depth and with the averaged wind-driven horizontal water transport at a right angle to the wind direction (Image credit: NOAA). (Colour online)

between the recorded data and classical Ekman theory. Since explicit solutions for non-constant eddy viscosity are very scarce (see Madsen 1977, Grisogno 1995, Constantin and Johnson 2019a), a general theoretical approach is needed to investigate Ekman flows with depth-dependent eddy viscosities. In this paper, we will establish the general validity of the characteristics (ii) and (iii) of Ekman flows by adapting and simplifiying the approach used in Constantin and Johnson (2019a) for flows in the atmospheric boundary layer. With regard to the deflection angle, for eddy viscosities that are small perturbations of a constant, we simplify the perturbative approach proposed in Bressan and Constantin (2019) to derive a formula that predicts the deviation of the deflection angle from the classical 45° reference value. In particular, this formula invalidates the speculation (see the discussion in Krauss 1993) that eddy viscosities that increase/decrease with depth produce deflection angles less/larger than 45°.

2. Preliminaries

The linear steady-state equations for the wind-induced current in the f-plane approximations are (see Wang and Huang 2004, Cronin and Kessler 2009)

$$-fv = \frac{\partial}{\partial z}\left(K(z)\frac{\partial u}{\partial z}\right), \qquad fu = \frac{\partial}{\partial z}\left(K(z)\frac{\partial v}{\partial z}\right), \tag{1a,b}$$

where (u, v) is the horizontal velocity vector, f is the vertical component of the Coriolis parameter, and $K(z)$ is the depth-dependent vertical eddy viscosity coefficient. The surface boundary condition,

$$(\tau_1, \tau_2) = \rho K(z)\left(\frac{\partial u}{\partial z}, \frac{\partial v}{\partial z}\right) \qquad \text{at the surface} \qquad z = 0, \tag{2}$$

relates the wind-stress vector (τ_1, τ_2) with the shear stress, ρ being the (constant) density, while the bottom boundary conditions,

$$(u,\ v), \left(\frac{\partial u}{\partial z}, \frac{\partial v}{\partial z}\right) \to (0,0) \qquad \text{as} \qquad z \to -\infty, \tag{3}$$

express the fact that the wind-drift current is insignificant at great depths. Ekman's classical solution for constant eddy viscosity $K(z) = K_0 > 0$ in the non-equatorial Northern Hemisphere (for $f > 0$) is, in complex variables notation,

$$u + \mathrm{i}v = \frac{1}{\rho\sqrt{fK_0}}[\tau_1 + \mathrm{i}\tau_2]\, \mathrm{e}^{\lambda z}\, \mathrm{e}^{\mathrm{i}(\lambda z - \pi/4)}, \tag{4}$$

where

$$\lambda = \sqrt{\frac{f}{2K_0}}.$$

The wind-driven horizontal current $[u + \mathrm{i}v]$ is directed at 45° to the right of the wind stress $[\tau_1 + \mathrm{i}\tau_2]$, decays and rotates with depth to the right to form a spiral, while the depth-averaged mass transport per unit width attributed to the wind,

$$\int_{-\infty}^{0} \rho[u + \mathrm{i}v]\, \mathrm{d}z = \frac{-\mathrm{i}}{f}[\tau_1 + \mathrm{i}\tau_2],$$

is at right angles to the wind stress (see figure 1). In contrast to the case of constant eddy viscosity, one can not expect to validate the counterparts of the three main characteristics of the classical Ekman flow by means of explicit calculations. In this paper, we address the case of eddy viscosities $K(z)$ that are perturbations of an asymptotic reference value $K_0 = \lim_{z\to-\infty} K(z) > 0$, so that

$$K(z) = K_0 + \varepsilon K_1(z) + \mathrm{o}(\varepsilon) > 0, \quad z \le 0, \tag{5}$$

where $\varepsilon \ll 1$ and K_1, K_1' are bounded on $(-\infty, 0]$.

3. Depth-averaged mass transport and the general Ekman spiral

The general validity of the depth-averaged mass transport per unit width being at right angles to the wind stress follows at once by integrating (1) and taking (2) into account:

$$\int_{-\infty}^{0} \rho[u + \mathrm{i}v]\, \mathrm{d}z = \frac{-\rho\mathrm{i}}{f}\left\{K(z)\left[\frac{\partial u}{\partial z} + \mathrm{i}\,\frac{\partial u}{\partial z}\right]\right\}_{z=0} = \frac{-\mathrm{i}}{f}\,[\tau_1 + \mathrm{i}\tau_2].$$

We now claim that *for a general depth-dependent eddy viscosity the horizontal current velocity vectors form a descending spiral to the right/left direction of the wind in the non-equatorial Northern/Southern Hemisphere, with a decreasing speed as the depth increases* (see figure 2).

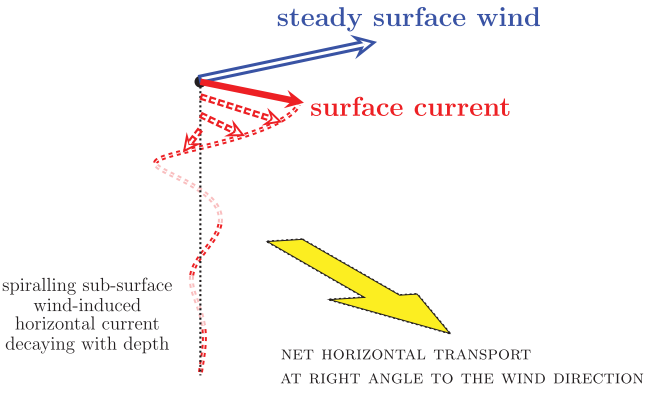

Figure 2. For a depth-dependent eddy viscosity the wind-induced horizontal current in the Northern Hemisphere spirals to the right of the wind direction and decays with increasing depth, with the wind-driven horizontal transport oriented perpendicular to the direction of the wind, a qualitative pattern predicted by Ekman's classical theory. However, the angle between the surface current and the wind direction is found often to differ substantially from the 45° reference value of the classical theory. (Colour online)

To prove this claim, it is convenient to introduce polar coordinates. We denote the flow speed by

$$M(z) = \sqrt{u^2(z) + v^2(z)} \geq 0, \quad z \leq 0,$$

and let θ with $\theta(0) := \theta_0 \in (-\pi, \pi]$ be such that

$$u(z) = M(z)\cos\big(\theta(z)\big), \qquad v(z) = M(z)\sin\big(\theta(z)\big), \quad z \leq 0. \tag{6a,b}$$

Then M is differentiable whenever $M \neq 0$ and

$$u' = M'\cos\theta - M\theta'\sin\theta, \qquad v' = M'\sin\theta + M\theta'\cos\theta, \tag{7a,b}$$

where the $'$ stands (here and henceforth) for the z-derivative, while

$$u'' = M''\cos\theta - 2M'\theta'\sin\theta - M\theta''\sin\theta - M\,(\theta')^2\cos\theta, \tag{8a}$$

$$v'' = M''\sin\theta + 2M'\theta'\cos\theta + M\theta''\cos\theta - M(\theta')^2\sin\theta, \tag{8b}$$

so that (1) is replaced by the pair of equations

$$\begin{aligned}
&[K'M' + KM'' - KM(\theta')^2]\cos\theta \\
&\qquad - [(K'M + 2KM')\theta' + KM\theta'']\sin\theta = -f\,M\sin\theta, \\
&[K'M' + KM'' - KM(\theta')^2]\sin\theta \\
&\qquad + [(K'M + 2KM')\theta' + KM\theta'']\cos\theta = f\,M\cos\theta.
\end{aligned}$$

In the above system, multiply the first equation by $\cos\theta$ and add to the second equation multiplied by $\sin\theta$, and then multiply the first equation by $-M\sin\theta$ and add to the second equation multiplied by $M\cos\theta$ to obtain the nonlinear system

$$KM'' + K'M' - KM(\theta')^2 = 0, \tag{9a}$$

$$(KM^2\theta')' = fM^2, \tag{9b}$$

which is equivalent to (1) on the subintervals of $(-\infty, 0]$ where $M \neq 0$; we will actually prove that $M(0) > 0$ ensures $M(z) > 0$ for all $z \leq 0$. The boundary conditions (2) and (3) are transformed to

$$M'(0)\cos\theta_0 - M(0)\theta'(0)\sin\theta_0 = \frac{1}{\rho K(0)}\tau_1, \tag{10a}$$

$$M'(0)\sin\theta_0 + M(0)\theta'(0)\cos\theta_0 = \frac{1}{\rho K(0)}\tau_2, \tag{10b}$$

and

$$M, \sqrt{(M')^2 + (M\theta')^2} \to 0 \qquad \text{as} \qquad z \to -\infty, \tag{11}$$

respectively. Multiplying the first equation in (10) by $\cos\theta_0$ and adding to the second equation multiplied by $\sin\theta_0$, and then multiplying the first equation by $-\sin\theta_0$ and adding to the second equation multiplied by $\cos\theta_0$, we transform (10) into

$$M'(0) = \frac{\alpha}{\rho K(0)}\cos(\beta - \theta_0), \qquad M(0)\theta'(0) = \frac{\alpha}{\rho K(0)}\sin(\beta - \theta_0), \tag{12a,b}$$

where $\alpha = \sqrt{\tau_1^2 + \tau_2^2} > 0$ and $\beta \in (-\pi, \pi]$ are such that

$$\tau_1 = \alpha\cos\beta, \qquad \tau_2 = \alpha\sin\beta. \tag{13a,b}$$

Here β is the direction of the wind at the surface, while α is the strength of the wind-stress; typically $(\tau_1, \tau_2) = c_D\rho_{\text{air}}U_{\text{wind}}|U_{\text{wind}}|$, where U_{wind} is the wind velocity at 10 m above the sea surface, ρ_{air} is the density of air (about 1.2 kg m^{-3}) and $c_D \approx 0.0013$ is a dimensionless drag coefficient (see the discussion in Wenegrat *et al.* 2014).

For constant eddy viscosity $K = K_0$, Ekman's classical solution (4) corresponds to the solution of the system (9) with the boundary conditions (11) and (12):

$$M(z) = M_0\,\mathrm{e}^{\lambda z}, \qquad \theta(z) = \theta_0 + \frac{f}{|f|}\lambda z, \tag{14a,b}$$

for $z \leq 0$, where

$$\lambda = \sqrt{|f|/(2K_0)}, \qquad \theta_0 = \beta - \frac{f}{|f|}\frac{\pi}{4}, \qquad M_0 = \frac{\alpha}{\rho\sqrt{|f|K_0}}. \tag{15a-c}$$

For a general depth-dependent eddy viscosity $K(z)$, writing (9a) as

$$(KM')' = KM(\theta')^2 \geq 0$$

and taking into account the fact that $KM' \to 0$ for $z \to -\infty$ is ensured by (11), we deduce that $M'(z) \geq 0$ for all $z \leq 0$. Let us now show that $M(z) > 0$ for all $z \leq 0$, assuming $M \not\equiv 0$. Indeed, the existence of some $z_0 < 0$ with $M(z_0) = 0$ would force $M(z) = 0$ for all $z \leq z_0$, in particular $M(z_0) = M'(z_0) = 0$. But then, interpreting (9a) as a second-order ordinary differential equation in M, the existence and uniqueness theorem yields $M \equiv 0$. Consequently, we infer that $M(z) > 0$ for all $z \leq 0$.

To investigate the general behaviour of θ, without loss of generality, we discuss the case of a non-equatorial region within the Northern Hemisphere, the case of the Southern Hemisphere being analogous. Equation (9b) yields for $f > 0$ that the function $KM^2\theta'$ is strictly increasing on $(-\infty, 0]$. We aim to prove that $\theta'(z) > 0$ for all $z < 0$, so that the spiralling of the horizontal velocity is always clockwise and never stops as one descends into the fluid. Assume $\theta'(z_0) \leq 0$ for some $z_0 \leq 0$. Then, since $KM^2\theta'$ is strictly increasing on $(-\infty, 0]$, we must have $\theta'(z) < 0$ for $z < z_0$. Fixing some $z^* < z_0$ and denoting

$$A = K(z^*)M^2(z^*)\theta'(z^*) < 0,$$

we have

$$K(z)M^2(z)\theta'(z) \leq A < 0, \quad z \leq z^*,$$

and therefore (9a) yields

$$\begin{aligned} K'(z)M'(z) + K(z)M''(z) &= K(z)M(z)[\theta'(z)]^2 \\ &= [K(z)M^2(z)\theta'(z)]^2 \frac{1}{K(z)M^3(z)} \\ &\geq A^2 \frac{1}{K(z)M^3(z)} \qquad \text{for} \qquad z \leq z^*. \end{aligned}$$

Multiplying both sides of the above inequality by $2K(z)M'(z) \geq 0$ leads us to

$$2K(z)M'(z)[K(z)M'(z)]' \geq A^2 \frac{2M'(z)}{M^3(z)} \qquad \text{for} \qquad z \leq z^*,$$

and an integration on $[z, z^*]$ yields

$$[K(z^*)M'(z^*)]^2 - [K(z)M'(z)]^2 \geq A^2 \left(\frac{1}{M^2(z)} - \frac{1}{M^2(z^*)} \right) \quad \text{for} \quad z < z^*.$$

In the limit $z \to -\infty$ of the above inequality we obtain a contradiction, since the left-hand side converges to $[K(z^*)M'(z^*)]^2$, while the right-hand side blows-up because $\lim_{z\to-\infty} M(z) = \lim_{z\to-\infty} M'(z) = 0$ and $K(z)$ is bounded. The obtained contradiction enables us to conclude that $\theta'(z) > 0$ for all $z < 0$. This proves our claim.

4. The deflection angle at the surface: a perturbative approach

Introducing the complex-valued function $\Psi(z) = u(z) + \mathrm{i}v(z)$, we can write the system (1) more compactly as the complex-valued second order differential equation

$$(K\Psi')' = \mathrm{i}f\,\Psi, \quad z < 0, \tag{16}$$

and we recast the boundary conditions (2) and (3) as

$$\Psi'(0) = \frac{1}{\rho K(0)}[\tau_1 + \mathrm{i}\tau_2], \tag{17a}$$

$$\Psi, \Psi' \to 0 \qquad \text{for} \qquad z \to -\infty. \tag{17b}$$

Writing

$$\Psi(z) = \Psi_0(z) + \varepsilon\Psi_1(z) + \mathrm{o}(\varepsilon), \quad z \le 0, \tag{18}$$

where Ψ_0 is the classical Ekman solution for the constant eddy viscosity K_0, and inserting (18) into (17), using (5), one obtains

$$K_0\Psi_1'' + K_1'\Psi_0' + K_1\Psi_0'' = \mathrm{i}f\Psi_1 + \mathrm{o}(\varepsilon). \tag{19}$$

For the non-equatorial Northern Hemisphere, from (4) we get

$$\Psi_0' = \sqrt{\frac{f}{2K_0}}\,(1+\mathrm{i})\Psi_0, \qquad \Psi_0'' = \frac{\mathrm{i}f}{K_0}\,\Psi_0,$$

so that letting $\varepsilon \to 0$ in (19) yields a linear, non-homogeneous second-order differential equation for the perturbation Ψ_1, namely

$$\Psi_1'' - \mathrm{i}\frac{f}{K_0}\Psi_1 = b \tag{20}$$

with

$$b(z) = -\left((1+\mathrm{i})K_1'(z)\sqrt{\frac{f}{2K_0^3}} + K_1(z)\frac{\mathrm{i}f}{K_0^2}\right)\Psi_0(z), \tag{21}$$

to be solved with homogeneous boundary and asymptotic conditions

$$\Psi_1'(0) = 0, \qquad \Psi_1 \to 0 \ \text{ for } z \to -\infty. \tag{22}$$

Note that if $\Psi_1 \to 0$ for $z \to -\infty$, then the fact that $\Psi_0 \to 0$ for $z \to -\infty$, in combination with (20) and the boundedness of K_1 and K_1', yield $\Psi_1'' \to 0$ for $z \to -\infty$, which forces $\Psi_1' \to 0$ for $z \to -\infty$. Indeed, if for a fixed $z_0 \le 0$ we define

$$m_0 = \sup_{z\le z_0}\{|\Psi_1(z)|\}, \qquad m_1 = \sup_{z\le z_0}\{|\Psi_1'(z)|\}, \qquad m_2 = \sup_{z\le z_0}\{|\Psi_1''(z)|\},$$

then $m_1^2 \le 4m_0m_2$ (see Rudin 1976). This explains why the asymptotic condition $\Psi_1' \to 0$ for $z \to -\infty$, required in (17), is automatically granted if the asymptotic condition in (22) holds.

Writing (20) in the form of the first-order differential system $\Phi' = \mathcal{A}\Phi + \mathcal{B}$, where

$$\Phi = \begin{pmatrix}\Psi_1\\ \Psi_1'\end{pmatrix}, \qquad \mathcal{A} = \begin{pmatrix}0 & 1\\ \dfrac{\mathrm{i}f}{K_0} & 0\end{pmatrix}, \qquad \mathcal{B} = \begin{pmatrix}0\\ b\end{pmatrix},$$

the variation of constants formula yields a representation of the general solution in the form

$$\Phi(z) = \mathrm{e}^{\mathcal{A}z}\Phi(0) - \int_z^0 \mathrm{e}^{\mathcal{A}(z-s)}\mathcal{B}(s)\,\mathrm{d}s, \quad z \le 0,$$

where

$$\begin{pmatrix} \frac{1}{2}\left[\mathrm{e}^{(1+\mathrm{i})\lambda z}+\mathrm{e}^{-(1+\mathrm{i})\lambda z}\right] & \frac{1}{2(1+\mathrm{i})\lambda}\left[\mathrm{e}^{(1+\mathrm{i})\lambda z}-\mathrm{e}^{-(1+\mathrm{i})\lambda z}\right] \\ \frac{(1+\mathrm{i})\lambda}{2}\left[\mathrm{e}^{(1+\mathrm{i})\lambda z}-\mathrm{e}^{-(1+\mathrm{i})\lambda z}\right] & \frac{1}{2}\left[\mathrm{e}^{(1+\mathrm{i})\lambda z}+\mathrm{e}^{-(1+\mathrm{i})\lambda z}\right] \end{pmatrix}, \quad z\in\mathbb{R},$$

is the fundamental matrix of the homogeneous constant-coefficient differential system $\Phi' = \mathcal{A}\Phi$. Since $\Psi_1'(0) = 0$, we get

$$\begin{aligned}\Psi_1(z) = {} & \frac{1}{2}\left[\mathrm{e}^{(1+\mathrm{i})\lambda z}+\mathrm{e}^{-(1+\mathrm{i})\lambda z}\right]\Psi_1(0) \\ & -\int_z^0 \frac{\mathrm{e}^{(1+\mathrm{i})\lambda(z-s)}-\mathrm{e}^{-(1+\mathrm{i})\lambda(z-s)}}{2(1+\mathrm{i})\lambda}\, b(s)\,\mathrm{d}s, \quad z\le 0, \end{aligned} \tag{23}$$

with $\Psi_1(0)$ to be chosen so that the asymptotic condition $\lim_{z\to-\infty}\Psi_1(z) = 0$ from (22) holds. Clearly

$$\lim_{z\to-\infty} \tfrac{1}{2}\mathrm{e}^{(1+\mathrm{i})\lambda z}\,\Psi_1(0) = 0,$$

while the Lebesgue dominated convergence theorem (see Rudin 1976) yields

$$\lim_{z\to-\infty} \frac{1}{2(1+\mathrm{i})\lambda}\int_z^0 \mathrm{e}^{(1+\mathrm{i})\lambda(z-s)} b(s)\,\mathrm{d}s = 0,$$

since b is integrable on $(-\infty, 0]$ and $|\mathrm{e}^{(1+\mathrm{i})\lambda(z-s)}| \le 1$ for $s \ge z$. Consequently, writing (23) as

$$\begin{aligned}\Psi_1(z) = {} & \tfrac{1}{2}\mathrm{e}^{(1+\mathrm{i})\lambda z}\,\Psi_1(0) - \frac{1}{2(1+\mathrm{i})\lambda}\int_z^0 \mathrm{e}^{(1+\mathrm{i})\lambda(z-s)} b(s)\,\mathrm{d}s \\ & + \frac{1}{2}\,\mathrm{e}^{-(1+\mathrm{i})\lambda z}\left[\Psi_1(0) + \frac{1}{(1+\mathrm{i})\lambda}\int_z^0 \mathrm{e}^{(1+\mathrm{i})\lambda s} b(s)\,\mathrm{d}s\right], \quad z\le 0, \end{aligned}$$

for the asymptotic condition in (22) to hold, we must have

$$\Psi_1(0) = -\frac{1}{(1+\mathrm{i})\lambda}\int_{-\infty}^0 \mathrm{e}^{(1+\mathrm{i})\lambda s}\, b(s)\,\mathrm{d}s. \tag{24}$$

Moreover, if (24) holds, then l'Hospital's rule in combination with (4) and (21) ensure

$$\lim_{z\to-\infty} \mathrm{e}^{-(1+\mathrm{i})\lambda z}\left[\Psi_1(0) + \frac{1}{(1+\mathrm{i})\lambda}\int_{-\infty}^0 \mathrm{e}^{(1+\mathrm{i})\lambda s}\, b(s)\,\mathrm{d}s\right] = 0,$$

validating the asymptotic condition in (22).

From (18), (4) and (24), we obtain

$$\begin{aligned}\Psi(0) = {} & \frac{1}{\rho\sqrt{fK_0}}[\tau_1 + i\tau_2]\,\mathrm{e}^{-\mathrm{i}\pi/4} \\ & \times\left[1 + \varepsilon\frac{1}{K_0}\int_{-\infty}^0 \mathrm{e}^{2(1+\mathrm{i})\lambda s}\left(K_1'(s) + (1+\mathrm{i})\lambda K_1(s)\right)\mathrm{d}s\right], \end{aligned}$$

and an integration by parts permits us to re-arrange the integral expression, obtaining

$$\Psi(0) = \frac{1}{\rho\sqrt{fK_0}}[\tau_1 + i\tau_2]\,\mathrm{e}^{-\mathrm{i}\pi/4} \times \left[1 + \varepsilon\frac{1}{K_0}\left(K_1(0) - (1+\mathrm{i})\lambda\int_{-\infty}^{0}\mathrm{e}^{2(1+\mathrm{i})\lambda s}K_1(s)\,\mathrm{d}s\right)\right].$$

The complex variables formula

$$\frac{\mathrm{d}}{\mathrm{d}\varepsilon}\arg(1+\varepsilon\xi)\bigg|_{\varepsilon=0} = \mathrm{Im}\{\xi\}$$

enables us to express the change of the deflection angle due to the perturbation as

$$\mathrm{Im}\left\{-\frac{(1+\mathrm{i})\lambda}{K_0}\int_{-\infty}^{0}\mathrm{e}^{2(1+\mathrm{i})\lambda s}K_1(s)\,\mathrm{d}s\right\} = -\frac{\lambda\sqrt{2}}{K_0}\int_{-\infty}^{0}\mathrm{e}^{2\lambda s}K_1(s)\sin\left(2\lambda s+\frac{\pi}{4}\right)\mathrm{d}s. \tag{25}$$

Due to (25), a positive/negative value of the integral $\int_{-\infty}^{0}\mathrm{e}^{2\lambda s}K_1(s)\sin(2\lambda s+\pi/4)\,\mathrm{d}s$ corresponds to an increase/decrease of the deflection angle from the reference value $\pi/4$.

The formula (25) is analogous to a formula derived recently in Bressan and Constantin (2019) in terms of the implicit variable $t(z) = K_0\int_0^z[K(s)]^{-1}\,\mathrm{d}s$. Despite their similarity – due to a typographical error, a multiplicative minus factor is actually missing on both sides of formula (22) in Bressan and Constantin (2019) – the formula (25) is advantageous since it is expressed in terms of the physical depth variable z, rather than implicitly (as in Bressan and Constantin 2019).

For example, let us consider for $K_0 > 0 > z_0$ and $\mu > 0$ the piecewise linear eddy viscosity

$$K(z) = \begin{cases} \mu + \dfrac{K_0-\mu}{z_0}z, & z_0 \le z \le 0, \\ K_0, & z < z_0, \end{cases} \tag{26}$$

that is decreasing or increasing with depth, according to whether $\mu > K_0$ or $\mu > K_0$, respectively. For (26), we have

$$\varepsilon K_1(z) = \begin{cases} \dfrac{K_0-\mu}{z_0}(z-z_0), & z_0 \le z \le 0, \\ 0, & z < z_0, \end{cases}$$

so that the integral in (25) becomes

$$\mathfrak{I} = \frac{K_0-\mu}{z_0}\left[\int_{z_0}^{0}s\mathrm{e}^{2\lambda s}\sin\left(2\lambda s+\frac{\pi}{4}\right)\mathrm{d}s - z_0\int_{z_0}^{0}\mathrm{e}^{2\lambda s}\sin\left(2\lambda s+\frac{\pi}{4}\right)\mathrm{d}s\right].$$

Since

$$\left[\frac{1}{2\lambda\sqrt{2}}\mathrm{e}^{2\lambda s}\sin(2\lambda s)\right]' = \mathrm{e}^{2\lambda s}\sin\left(2\lambda s+\frac{\pi}{4}\right), \tag{27a}$$

$$\left[\frac{1}{2\lambda\sqrt{2}}\,\mathrm{e}^{2\lambda s}\sin\left(2\lambda s-\frac{\pi}{4}\right)\right]'=\mathrm{e}^{2\lambda s}\sin(2\lambda s), \tag{27b}$$

we can use integration by parts and the fundamental theorem of calculus to compute

$$\begin{aligned}\mathfrak{I}&=\frac{K_0-\mu}{z_0}\left[\frac{s}{2\lambda\sqrt{2}}\,\mathrm{e}^{2\lambda s}\sin(2\lambda s)\Big|_{s=z_0}^{s=0}\right.\\&\qquad\left.-\frac{1}{2\lambda\sqrt{2}}\int_{z_0}^{0}\mathrm{e}^{2\lambda s}\sin(2\lambda s)\,\mathrm{d}s-\frac{z_0}{2\lambda\sqrt{2}}\,\mathrm{e}^{2\lambda s}\sin(2\lambda s)\Big|_{s=z_0}^{s=0}\right]\\&=-\frac{K_0-\mu}{z_0}\frac{1}{2\lambda\sqrt{2}}\int_{z_0}^{0}\mathrm{e}^{2\lambda s}\sin(2\lambda s)\,\mathrm{d}s\\&=-\frac{K_0-\mu}{z_0}\frac{1}{8\lambda^2}\,\mathrm{e}^{2\lambda s}\sin\left(2\lambda s-\frac{\pi}{4}\right)\Big|_{s=z_0}^{s=0}\\&=\frac{K_0-\mu}{z_0}\frac{1}{8\lambda^2}\left[\frac{1}{\sqrt{2}}+\mathrm{e}^{2\lambda z_0}\sin\left(2\lambda z_0-\frac{\pi}{4}\right)\right].\end{aligned}$$

In view of (25), this shows that whether the deflection angle is smaller or larger than 45° is determined not by the monotonicity of K but by the values of the depth $|z_0|$ of the near-surface region of non-constant eddy viscosity and of the surface eddy viscosity μ. This invalidates the expectation (arising from the case study Madsen 1977) of a linear decrease with depth (see the discussion in Krauss 1993) that an eddy viscosity that increases/decreases with depth produces a deflection angle that lags/exceeds 45°. Note that the approach in Bressan and Constantin (2019) also applies to (26), but the conclusion is less precise due to the intricate nature of the implicit alternative to the formula (25).

5. Discussion

Throughout the research literature various choices of depth-dependent eddy viscosities are investigated. The corresponding Ekman-type solutions all retain two of the fundamental properties of the classical, constant eddy-viscosity, Ekman flow: the depth-averaged mass flow (Ekman transport) is at right angles to the steady wind at the surface and the horizontal wind-induced current spirals to the right in the Northern Hemisphere, with a speed that decreases with increasing depth. On the other hand, the deflection angle of the surface current with respect to the direction of the steady wind presents significant deviations from the reference value of 45° of the classical Ekman flow. This issue is especially relevant for the climate, since the ocean stores most of the heat in its near-surface region. It is therefore of interest to investigate the frictional effects for a general depth-dependent eddy viscosity. While the direction of the Ekman transport can be established generally by means of a simple computation (see the first paragraph of section 3), the other aspects are more challenging.

In section 3, we have adapted an approach that was used recently in Constantin and Johnson (2019a) in the study of the atmospheric boundary layer to the context of ocean flows. For a general variable eddy viscosity, we have shown that, in the Northern Hemisphere, the wind-induced horizontal current always decays in magnitude and turns

clockwise with increasing depth. This result is new, as all previous work was based on a few cases, corresponding to rather limited types of eddy viscosities, for which explicit calculations are possible.

In section 4, we have derived the formula (25) for the deviation of the deflection angle from the 45° reference value, for small perturbations of a constant leading-order eddy viscosity. This formula improves the recent result in Bressan and Constantin (2019) and, applied to the case of a piecewise linear eddy viscosity, invalidates the speculation that an eddy viscosity that increases/decreases with depth produces deflection angles less/larger than 45°. One can actually pursue a general investigation of the formula (25). Indeed, as s decreases from 0 towards $-\infty$, the function $\mathrm{e}^{2\lambda s}K_1(s)\sin(2\lambda s+\pi/4)$ changes sign alternately, being positive for $s\in I_0:=(-\pi/(8\lambda),0)$, negative on the intervals

$$I_{2j+1}:=\left(-\frac{\pi}{8\lambda}-\frac{\pi}{2\lambda}(2j+1),\frac{3\pi}{8\lambda}-\frac{\pi}{2\lambda}(2j+1)\right)$$

and positive on the intervals

$$I_{2j+2}:=\left(-\frac{\pi}{8\lambda}-\frac{\pi}{2\lambda}(2j+2),\frac{3\pi}{8\lambda}-\frac{\pi}{2\lambda}(2j+2)\right),$$

for integers $j\geq 0$. Moreover, using (27), we compute

$$\int_{I_0}\mathrm{e}^{2\lambda t}\sin\left(2\lambda t+\frac{\pi}{4}\right)\mathrm{d}t=\frac{\mathrm{e}^{-\pi/4}}{4\lambda},$$

$$\int_{I_{2j+1}}\mathrm{e}^{2\lambda t}\sin\left(2\lambda t+\frac{\pi}{4}\right)\mathrm{d}t=-\frac{\mathrm{e}^{-2\pi j}\left(\mathrm{e}^{-\pi/4}+\mathrm{e}^{-5\pi/4}\right)}{4\lambda},\quad j\geq 0,$$

$$\int_{I_{2j+2}}\mathrm{e}^{2\lambda t}\sin\left(2\lambda t+\frac{\pi}{4}\right)\mathrm{d}t=\frac{\mathrm{e}^{-2\pi j}\left(\mathrm{e}^{-5\pi/4}+\mathrm{e}^{-9\pi/4}\right)}{4\lambda},\quad j\geq 0,$$

and see that the sequence $\{E_m\}_{m\geq 0}$ of the absolute values of these integrals converges exponentially fast to zero and is strictly decreasing starting with $m\geq 1$, whereas

$$E_2\approx\frac{0.005}{\lambda}<E_0\approx\frac{0.114}{\lambda}<E_1\approx\frac{0.119}{\lambda}.$$

Taking K_1 to be constant of each of the intervals I_m shows that the key to whether the integral in (25) is positive or negative lies in the relative sizes of the values assigned to the intervals I_0 and I_1. Note that π/λ is the depth of the classical Ekman layer $\mathcal{L}$, the near-surface region of the ocean affected by the movement of wind and frictional influence (typically about 30–200 m deep), at the bottom of which the wind-induced current velocity is in the opposite direction to the surface current. Consequently, I_0 corresponds to the upper eighth part of $\mathcal{L}$, while I_1 extends to the lower half of the Ekman layer. In general, a slow and gradual variation of the eddy viscosity with depth will result in a positive integral $\mathfrak{I}$ (and thus a deflection angle larger than 45°), while if the eddy viscosity within I_0 is lower than within I_1, then the negative contribution from I_1 will dominate the positive on from I_0, with a negative integral $\mathfrak{I}$ as the typical outcome (and thus a deflection angle below 45°). Since an ice cover quells the turbulence near the ocean surface, this explains why the deflection angle is less than 45° in arctic regions. A further interesting application of formula (25)

regards the observation that the deviation of the surface current from the wind is typically larger during the day that during night-time (see Krauss 1993). Solar heating quenches turbulence throughout the near-surface layer during daytime since the induced slight but gradual change of density (with the lighter fluid above heavier fluid) hinders vertical mixing. On the other hand, turbulence becomes stronger at night due to nocturnal convection since the ocean's upper 100 m coincide with the depth above which the downward flux of solar energy exceeds 1% of the heat flux at the sea surface (see Woods 2002). The nocturnal increase of the eddy viscosity occurs across the upper half of the Ekman layer, with the change in the lower regions being rather insignificant, as the heat flux fades. This feature amplifies the contribution from the region I_1, leading thus typically to an overall negative integral in (25), so that the deflection angle is smaller during the night. The same argument applies to the large seasonal variations of the deflection angle observed at some locations. For example, in the Tsushima Strait the deflection angle is 17.7°–27.3° in winter and increases to 48.5°–67.3° in summer (see the data in Yoshikawa and Masuda 2009).

Formula (25), predicting the deviation of the deflection angle from the classical 45° reference value, can be regarded as a mathematical synthesis of various cases that could be studied individually, typically using numerical methods. The fact that (25) was derived rigorously for a clearly specified class of eddy viscosities prevents potentially misleading speculations based solely on the insight developed by computational methods. However, the validity of formula (25) is restricted to the class of small perturbations of a constant vertical eddy viscosity. It is of interest to go beyond this setting. For example, the case of piecewise uniform diffusivities can be examined in detail without the smallness assumptions inherent to a perturbative approach (see Dritschel *et al.* 2020).

Acknowledgments

The author is grateful for helpful comments from the referees.

Disclosure statement

No potential conflict of interest was reported by the author.

Funding

The support of the Vienna Science and Technology Fund (WWTF) grant MA16-009 is acknowledged.

References

Basu, B., Some numerical investigations into a nonlinear three-dimensional model of the Pacific equatorial ocean flows. *Deep Sea Res. II* 2019, **160**, 7–15.

Boyd, J.P., *Dynamics of the Equatorial Ocean*, 2018 (Springer: Berlin).

Bressan, A. and Constantin, A., The deflection angle of surface ocean currents from the wind direction. *J. Geophys. Res.: Oceans* 2019, **124**, 7412–7420.

Constantin, A. and Johnson, R.S., Atmospheric Ekman flows with variable eddy viscosity. *Boundary Layer Meteorol.* 2019a, **170**, 395–414.

Constantin, A. and Johnson, R.S., Ekman-type solutions for shallow-water flows on a rotating sphere: A new perspective on a classical problem. *Phys. Fluids* 2019b, **31**, 021401.

Constantin, A. and Johnson, R.S., On the nonlinear, three-dimensional structure of equatorial oceanic flows. *J. Phys. Oceanogr.* 2019c, **49**, 2029–2042.

Cronin, M.F. and Kessler, W.S., Near-surface shear flow in the tropical Pacific Cold Tongue Front. *J. Phys. Oceanogr.* 2009, **39**, 1200–1215.
Dritschel, D.G., Paldor, N. and Constantin, A. (2020). The Ekman spiral for piecewise uniform diffusivity.
Ekman, V.W., On the influence of the Earth's rotation on ocean-currents. *Ark. Mat. Astron. Fys.* 1905, **2**, 1–52.
Gill, A., *Atmosphere-Ocean Dynamics*, 2018 (Academic Press: New York).
Grisogno, B., A generalized Ekman layer profile with gradually varying eddy diffusivities. *Quart. J. Roy. Meteorol. Soc.* 1995, **121**, 445–453.
Henry, D., Nonlinear features of equatorial ocean flows. *Oceanography* 2018, **31**, 22–27.
Krauss, W., Ekman drift in homogeneous water. *J. Geophys. Res.* 1993, **98**, 187–209.
Levitus, S., Antonov, J.I., Boyer, T.P., Baranova, O.K., Garcia, H.E., Locarnini, R.A., Mishonov, A.V., Reagan, J.R., Seidov, D., Yarosh, E.S. and Zweng, M.M., World ocean heat content and thermosteric sea level change (0–2000 m), 1955–2010. *Geophys. Res. Lett.* 2012, **39**, L10603.
Madsen, O.S., A realistic model of the wind-induced Ekman boundary layer. *J. Phys. Oceanogr.* 1977, **7**, 248–255.
Marshall, J. and Plumb, R.A., *Atmosphere, Ocean and Climate Dynamics: An Introductory Text*, 2016 (Academic Press: New York).
Marshall, D. and Zanna, L., A conceptual model of ocean heat uptake under climate change. *J. Climate* 2014, **27**, 8444–8465.
Polton, J.A., Lenn, Y.-D., Elipot, S., Chereskin, T.K. and Sprintall, J., Can drake passage observations match Ekman's classic theory? *J. Phys. Oceanogr.* 2013, **43**, 1733–1740.
Roach, C.J., Phillips, H.E., Bindoff, N.L. and Rintoul, S.R., Detecting and characterizing Ekman currents in the Southern Ocean. *J. Phys. Oceanogr.* 2015, **45**, 1205–1223.
Roquet, F., Wunsch, C. and Madec, G., On the patterns of wind-power input to the ocean circulation. *J. Phys. Oceanogr.* 2011, **41**, 2328–2342.
Rudin, W., *Principles of Mathematical Analysis*, 1976 (McGraw-Hill Book Co.: New York).
Stacey, M.W., Pond, S. and Leblond, P.H.C., A wind-forced Ekman spiral as a good statistical fit to low-frequency currents in a coastal strait. *Science* 1986, **233**, 470–472.
Talley, L.D., Pickard, G.L., Emery, W.J. and Swift, J.H., *Descriptive Physical Oceanography: An Introduction*, 2011 (Academic Press: New York).
Vallis, G.K., *Atmospheric and Oceanic Fluid Dynamics*, 2005 (Cambridge University Press: Cambridge).
Viúdez, Á. and Dritschel, D.G., Vertical velocity in mesoscale geophysical flows. *J. Fluid Mech.* 2003, **483**, 199–223.
Wang, W. and Huang, R.X., Wind energy input to the Ekman layer. *J. Phys. Oceanogr.* 2004, **34**, 1267–1275.
Wenegrat, J.O., McPhaden, M.J. and Lien, R.-C., Wind stress and near-surface shear in the equatorial Atlantic Ocean. *Geophys. Res. Lett.* 2014, **41**, 1226–1231.
Woods, J., Laminar flow in the ocean Ekman layer. In *Meteorology at the Millenium*, edited by R.P. Pearce, pp. 220–232, 2002 (Academic Press: New York).
Yoshikawa, Y. and Masuda, A., Seasonal variations in the speed factor and deflection angle of the wind-driven surface flow in the Tsushima Strait. *J. Geophys. Res.* 2009, **114**, C12022.